Human Immunodeficiency Virus-1 Protease. 2. Use of pH Rate Studies and Solvent Kinetic Isotope Effects To Elucidate Details of Chemical Mechanism

Lawrence J. Hyland, Thaddeus A. Tomaszek, Jr., and Thomas D. Meek*

Department of Medicinal Chemistry, SmithKline Beecham Pharmaceuticals, 709 Swedeland Road, King of Prussia, Pennsylvania 19406

Received March 25, 1991; Revised Manuscript Received May 29, 1991

ABSTRACT: The pH dependence of the peptidolytic reaction of recombinant human immunodeficiency virus type 1 protease has been examined over a pH range of 3–7 for four oligopeptide substrates and two competitive inhibitors. The pK values obtained from the pK_{is} vs pH profiles for the unprotonated and protonated active-site aspartyl groups, Asp-25 and Asp-25′, in the monoprotonated enzyme form were 3.1 and 5.2, respectively. Profiles of log V/K vs pH for all four substrates were "bell-shaped" in which the pK values for the unprotonated and protonated aspartyl residues were 3.4–3.7 and 5.5–6.5, respectively. Profiles of log V vs pH for these substrates were "wave-shaped" in which V was shifted to a constant lower value upon protonation of a residue of pK = 4.2–5.2. These results indicate that substrates bind only to a form of HIV-1 protease in which one of the two catalytic aspartyl residues is protonated. Solvent kinetic isotope effects were measured over a pH(D) range of 3–7 for two oligopeptide substrates, Ac-Arg-Ala-Ser-Gln-Asn-Tyr-Pro-Val-Val-NH_2 and Ac-Ser-Gln-Asn-Tyr-Pro-Val-Val-NH_2. The pH-independent value for $^DV/K$ was 1.0 for both substrates, and ^DV = 1.5–1.7 and 2.2–3.2 at low and high pH(D), respectively. The attentuation of both V and ^DV at low pH(D) is consistent with a change in rate-limiting step from a chemical one at high pH(D) to one in which a product release step or an enzyme isomerization step becomes partly rate-limiting at low pH(D). Proton inventory data is in accord with the concerted transfer of two protons in the transition state of a rate-limiting chemical step in which the enzyme-bound amide hydrate adduct collapses to form the carboxylic acid and amine products.

The aspartic proteases of mammalian and fungal origin, such as pepsin, penicillopepsin, renin, and cathepsin D, are bilobal monomeric proteins of >30 kDa that contain at their active sites two eponymous aspartyl residues. From extensive structural and kinetic characterizations of these enzymes [for reviews, see Polgar (1989), Fruton (1987), Kostka (1985), and Tang (1977)], it is now clear that their active sites reside in a deep cleft formed at the interface of the two lobes, each lobe contributing one of two catalytic aspartyl residues located within an identical tripeptide sequence, Asp-Thr-Gly. The aspartyl groups are in opposite states of protonation, such that the catalytically competent form of these enzymes is a "monoprotonated" one. This conclusion is based on three-dimensional structural data of these enzymes, affinity labeling studies, and the observation of "bell-shaped" profiles of log V/K vs pH or log V vs pH for oligopeptide substrates of porcine pepsin (Clement et al., 1968; Cornish-Bowden & Knowles, 1969; Hunkapiller & Richards, 1972; Clement, 1973), penicillopepsin (Hofmann et al., 1984), and human renin (Green et al., 1990).

From considerations of sequence homology (Pearl & Taylor, 1987) and kinetic behavior (Meek et al., 1989), the retroviral protease of HIV-1[1] has many of the characteristics of the aspartic proteases but differs from these enzymes in that its active form is a homodimer of 11-kDa subunits (Meek et al., 1989). Recently, the solution of the three-dimensional structure of both recombinant (Navia et al., 1989; Lapatto et al., 1989) and synthetic (Wlodawer et al., 1989) HIV-1 protease has revealed that the overall molecular architecture of this enzyme is very similar to that of the monomeric aspartic proteases. For HIV-1 protease, each 99 amino acid subunit of the C-2 symmetric homodimer contributes (a) a glycine-rich loop (known as a "flap") that constitutes in part the substrate-binding sites of the enzyme and (b) one of two active-site aspartyl residues, Asp-25 and Asp-25′. The active-site aspartyl residues exist on opposite sides of the C-2 axis of symmetry present in the homodimeric protein. The structural configuration of the aspartyl residues within the active site formed at the dimeric interface is indistinguishable from those of the monomeric aspartic proteases. It is therefore reasonable to suggest that the aspartic proteases of retroviral and nonviral origin operate by similar chemical mechanisms.

Although many aspects of the chemical mechanism of the aspartic proteases remain unresolved, from recent structural analysis of enzyme–inhibitor complexes (Suguna et al., 1987; James & Sielecki, 1985; Bott et al., 1982) it is now widely believed that the active-site aspartyl groups assume opposite roles in general acid–general base catalysis, in which deprotonation of the lytic H_2O is performed by the unprotonated aspartyl residue and polarization (or protonation) of the scissile carbonyl oxygen is achieved by the protonated aspartyl residue. Given the structural similarities between the monomeric aspartic proteases and the retroviral proteases, we sought to characterize the chemical mechanism of HIV-1 protease by use of pH rate profiles of four oligopeptide substrates and two competitive inhibitors and by solvent kinetic isotope effects. These inhibitors are synthetic analogues of oligopeptide substrates that contain isosteric replacements for the scissile dipeptide amide bond: a "reduced amide" isostere (1; Moore

* Author to whom correspondence should be addressed.

[1] Abbreviations: Boc, *tert*-butyloxycarbonyl; DTT, dithiothreitol; EDTA, ethylenediaminetetraacetic acid; HIV-1, human immunodeficiency virus type 1; HPLC, high-performance liquid chromatography; Mes, 2-(*N*-morpholino)ethanesulfonic acid; Tris, tris(hydroxymethyl)aminomethane; amino acids are designated by the one-letter code.

0006-2960/91/0430-8454$02.50/0

et al., 1989) and a hydroxyethylene (cyclopentyl) isostere (**2**; Dreyer et al., 1989).

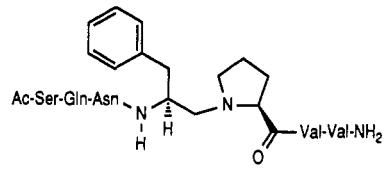

1

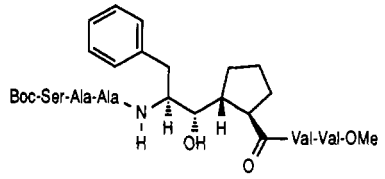

2

Experimental Procedures

Enzyme and Chemicals. Sources of purified recombinant HIV-1 protease and oligopeptide substrates were as described in the preceding paper in this issue. The "reduced amide" peptide analogue inhibitor **1** was prepared by reductive amination of the *N*-Boc-L-tyrosinal with proline methyl ester in the presence of sodium cyanoborohydride as previously described (Moore et al., 1989). The hydroxyethylene-containing inhibitor **2** has been previously described (Dreyer et al., 1989), and its synthesis will be described elsewhere (Dreyer et al., manuscript in preparation). Deuterium oxide (99.8–99.9 atom % D) was obtained from either MSD isotopes or Aldrich Chemicals (Gold Label). Glycerol (Ultrograde) was a product of LKB. All other chemicals were of the highest available quality.

Enzyme Assays. The following buffers were used for enzymatic assays: 50 mM 2-(*N*-morpholino)ethanesulfonic acid (Mes) (pH 6.0), 1 mM EDTA, 0.2 M NaCl, 1 mM dithiothreitol, and 0.1% (v/v) Triton X-100 (MENDT buffer); 50 mM each of glycine, sodium acetate, Mes, Tris-HCl (variable pH), 1 mM dithiothreitol, 1 mM EDTA, 0.2 M NaCl, and 0.1% (v/v) Triton X-100 (GAMT-NEDT buffer). In general, peptidolytic assays were conducted in 50-μL reaction mixtures that were maintained at 37 °C in a water-filled temperature-regulated heating block. Mixtures containing buffer, substrates (0.1–10 mM), and inhibitors were preincubated for 7–10 min at 37 °C prior to initiation of reaction by the addition of HIV-1 protease (room temperature). Reactions were quenched at various times ($t \leq 20$ min) by the addition of 50 μL of 3% (v/v) trifluoroacetic acid, and the samples were then analyzed by reverse-phase HPLC as outlined in the accompanying paper (Hyland et al., 1991).

(*a*) *pH Studies.* The pH dependence of V/K and V for the oligopeptide substrates AcSQNYPVV-NH_2, AcRASQNYPVV-NH_2, AcSQSYPVV-NH_2, and AcRKILFLDG-NH_2 and the apparent pK_i for product and dead-end inhibitors of HIV-1 protease were investigated over a pH range of 3–7 with a mixed buffer (GAMT-NEDT buffer) titrated to the indicated pH values (measured on an Orion 601A pH meter equipped with a Ross combination glass electrode) by the addition of HCl or NaOH. The ionic strength was held constant by adjusting each titrated reaction mixture to constant conductivity (approximately 20 millimhos) by the addition of small aliquots of 3 M NaCl. The pH and conductivity of each buffer were measured prior to determination of initial velocities. Values of V and V/K were determined from initial rates measured at 4–5 variable concentrations (0.1–10 mM) of the oligopeptide substrate at each value of pH, and substrate concentrations were at values equal to 0.2–2.0 times the Michaelis constant of the variable substrate. Reactions were initiated by the addition of HIV-1 protease [5–6 μL containing 18–24 ng (pH 4–7); 60–120 ng (pH 3–4)], and quenched at 5, 10, or 20 min, as described above. A reaction time course ($t \leq 20$ min) was determined at each pH value at a single substrate concentration to ensure uniformity in the enzymatic initial rates. Initial rate data were in most cases obtained from single time points ($t \leq 20$ min) at which substrate turnover was ≤18%, as described in the accompanying paper (Hyland et al., 1991).

Inhibitors **1** and **2** have been shown to be competitive inhibitors of the protease (Moore et al., 1989; Dreyer et al., 1989). The inhibition of HIV-1 protease by either **1** and **2** was determined at each value of pH between 3 and 7 from a double-reciprocal plot of inhibitor vs AcSQNYPVV-NH_2 under conditions as described above. The stability of the enzymatic activity of the protease over the operant pH range 3–7 was evaluated in the following manner: Protease (12 ng) was preincubated for 40 min at 37 °C in 15-μL solutions of 3× GAMT-NEDT buffer held at integral pH values of 2–9. Aliquots (5 μL) were then withdrawn and incubated (37 °C) in 25 μL of MENDT buffer (pH 6.0) containing 3 mM AcRASQNYPVV-NH_2 (final pH 5–6) to assess the remaining enzyme activity. The samples were quenched after 15 min, and enzymatic activity was analyzed as described above.

(*b*) *Solvent Kinetic Isotope Effects.* Solvent kinetic isotope effects on V and V/K for the oligopeptide substrates AcRASQNYPVV-NH_2, AcSQNYPVV-NH_2, and AcSQSYPVV-NH_2 were determined by measurement of peptidolytic initial rates at variable concentrations of these substrates in reaction mixtures composed of 88% (v/v) D_2O. The buffers used in these studies, MENDT buffer and GAMT-NEDT buffer, were prepared in D_2O and titrated with either DCl or NaOD to the indicated values of pD, where pD = $pH_{measured}$ + 0.33 for 88% D_2O (Schowen, 1977). Similarly, the oligopeptides substrates were prepared and quantified as described above in D_2O. Ionic strength was held to constant conductivity by the addition of small aliquots of 3 M NaCl dissolved in D_2O. For comparison of solvent kinetic isotope effects at a single value of pH(D), corresponding buffers were prepared in H_2O and D_2O in which pH was equal to pD. GAMT-NEDT [pH(D) 3–7] was used to investigate the pH(D) dependence of the solvent kinetic isotope effects for the substrates, AcSQNYPVV-NH_2 and AcRASQNYPVV-NH_2. As in the pH studies in H_2O, reactions (37 °C) were initiated by the addition of HIV-1 protease [18–24 ng (pD 3–4); 60–120 ng (pD 4–7)] and quenched after 5, 10, or 20 min as described. The reaction time course of the protease-catalyzed peptidolysis of AcRASQNYPVV-NH_2 exhibited linear behavior in 88% D_2O for at least 20 min (MENDT buffer, pD 6.0; GAMT-NEDT buffer, pD 3–7).

Proton inventories (Venkatasubban & Schowen, 1985; Schowen, 1978; Schowen, 1977) for the substrates AcRASQNYPVV-NH_2 and AcSQNYPVV-NH_2 were conducted at pH(D) 6 and 3.6 by determination of V/K and V for the substrates in MENDT (AcRASQNYPVV-NH_2) or GAMT-NEDT (AcSQNYPVV-NH_2) buffer at variable mole fractions of D_2O. Identical reaction mixtures, independently prepared in 100% H_2O and 100% D_2O, containing buffer and variable concentrations of peptide substrate, were combined to give variable mole fractions of D_2O (F_i = 0–0.97; final values). Following incubation at 37 °C, reactions were initiated by the addition of 18–24 ng of HIV-1 protease (5 μL) to the 45-μL

reaction mixtures, which were quenched (t = 5 or 20 min) and analyzed as described above.

Data Analysis. Kinetic data were fitted to the appropriate rate equations by using either the FORTRAN programs of Cleland (1979) or by using the SUPERFIT package, a nonlinear regression analysis utilizing the method of Marquardt (1983) and developed in-house. Values of V/K and V at changing pH or mole fraction of D_2O were obtained by fitting of initial velocity data at variable concentrations of the oligopeptide substrates to eq 1. In the equations that follow, v is the initial velocity, V is the maximum velocity, K is the Michaelis constant, and A is the concentration of variable substrate. The nomenclature used in the rate equations is that of Cleland (1963). Isotope effects are described in the text by the nomenclature of Northrop (1977), in which solvent kinetic isotope effects on kinetic parameters are denoted by the superscript D.

$$v = \frac{VA}{K + A} \tag{1}$$

Patterns conforming to linear competitive inhibition or linear noncompetitive inhibition were fitted to eqs 2 and 3, respectively.

$$v = \frac{VA}{K(1 + I/K_{is}) + A} \tag{2}$$

$$v = \frac{VA}{K(1 + I/K_{is}) + A(1 + I/K_{ii})} \tag{3}$$

Data for the pH (or pD) dependence of V/K and V for substrates or pK_{is} for inhibitors were fitted to eqs 4–8. Plots in which the log of the parameter decreased at acidic pH with a slope of 1 or 2 were fitted to eq 4 or 5, respectively. pH profiles in which the log of the plotted parameter decreased at acidic and basic pH with slopes of 1 and −1 were fitted to eq 6.

$$\log y = \log\left[\frac{c}{1 + H/K_1}\right] \tag{4}$$

$$\log y = \log\left[\frac{c}{1 + H/K_1 + H^2/K_1K_2}\right] \tag{5}$$

$$\log y = \log\left[\frac{c}{1 + H/K_1 + K_2/H}\right] \tag{6}$$

pH profiles that showed a plateau at high and low pH were fitted to eq 7. Profiles in which the log of the plotted parameter decreased with a slope of 1 at acidic pH but decreased with a slope of −1 to a lower "plateau" value at basic pH were fitted to eq 8.

$$\log y = \log\left[\frac{Y_L + Y_H(K_3'/H)}{1 + K_3'/H}\right] \tag{7}$$

$$\log y = \log\left[\frac{Y_L + Y_H(K_2/H)}{1 + H/K_1 + K_2/H}\right] \tag{8}$$

In eqs 4–8, y is the observed value of either V/K, V, or $1/K_{is}$; c is the pH-independent plateau value of y, Y_L, and Y_H are values of y at a plateau of low pH or high pH, respectively, H is the proton concentration, and K_1, K_2, and K_3', are apparent acid dissociation constants for groups on the enzyme, inhibitor, or substrate.

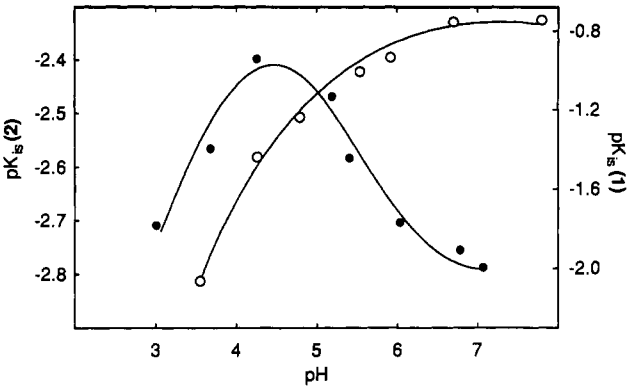

FIGURE 1: pH variation of the apparent slope inhibition constants (K_{is}) of inhibitors **1** (○) and **2** (●). The pK_{is} values were obtained from fitting of inhibitor vs AcSQNYPVV-NH_2 to eq 2 at each value of pH as described under Experimental Procedures. The curves drawn through the experimental data points are from fitting of the data to eqs 5 and 8 for inhibitor **1** and **2**, respectively.

For proton inventory studies, values of V/K and V at each mole fraction of D_2O (F_i) were obtained from eq 1. The proton inventory data of V vs F_i were then fitted individually to three forms of the Gross–Butler equation (eqs 9–11), which describe a transition state in which one (eq 9), two (eq 10), or three (eq 11) protons are transferred. V_{F_i} and V_{F0} are values of V measured at a mole fraction of D_2O of F_i or 0, respectively, and ϕ_n^T are the isotopic fractionation factors of individual hydrogenic positions (transferred protons) in the transition state in which n = 1, 2, or 3, as defined by Schowen (1978).

$$V_{F_i} = V_{F0}(1 - F_i + F_i\phi_1^T) \tag{9}$$

$$V_{F_i} = V_{F0}(1 - F_i + F_i\phi_1^T)(1 - F_i + F_i\phi_2^T) \tag{10}$$

$$V_{F_i} = V_{F0}(1 - F_i + F_i\phi_1^T)(1 - F_i + F_i\phi_2^T)(1 - F_i + F_i\phi_3^T) \tag{11}$$

When the type of kinetic pattern was in doubt for an experiment, data were fitted to all of the appropriate equations, and a comparison of the resulting σ values (square root of the average residual least square, for eqs 1, 2–4, and 6–7) or the correlation coefficients (eqs 5 and 8–11) were used to determine the best fit.

Results

pH(D) Studies. The pH stability of the enzymatic activity of HIV-1 protease was determined from the peptidolytic activity remaining at its optimal pH (5–6) following a 40-min preincubation at pH values of 2–9. Upon normalization of values to the sample preincubated at pH 6.0, 87–100% of the initial protease activity remained in samples preincubated at pH 3–7, while 1–4% of the activity was present in samples treated at pH 2 and 8–9. Thus, the enzyme activity is stable to pH values of 3–7 under standard assay conditions.

(*a*) *Competitive Inhibitors.* The pH dependence of pK_{is} for the two competitive inhibitors **1** and **2** were determined at pH 3–7 from double-reciprocal plots of inhibitor vs Ac-SQNYPVV-NH_2. Neither inhibitor possesses a titratable group in this pH range (the tertiary amine group of compound **1** would be protonated at pH ≤8), indicating that pK values which occur in these patterns should reflect groups on the protease. Either inhibitor was linear competitive at each value of pH as judged from a comparison of fitting of each data set to eqs 2 and 3. The resulting plots of pK_{is} vs pH for these inhibitors are shown in Figure 1.

For compound **1**, pK_{is} decreased at decreasing pH with a slope of 2. Fitting of these data to eq 5 indicated that two

Table I: pH(D) Rate Profiles for Oligopeptide Substrates and Inhibitors of HIV-1 Protease[a]

substrate or inhibitor	solvent	pH(D) range	kinetic parameter (y)	eq fitted	pK values and kinetic constants
inhibitor **1**	H_2O	3.5–7.1	K_{is}	5	$pK_1 = 3.1 \pm 0.1$, $pK_2 = 4.9 \pm 0.06$, $c = 5.5 \pm 0.3$ μM
inhibitor **2**	H_2O	3.0–7.1	K_{is}	8	$pK_1 = 3.3 \pm 0.1$, $pK_2 = 5.3 \pm 0.09$ $Y_L = 210 \pm 12$ nM, $Y_H = 680 \pm 27$ nM
AcSQNYPVV-NH_2	H_2O	3.2–6.1	V/K	6	$pK_1 = 3.57 \pm 0.08$, $pK_2 = 5.48 \pm 0.09$, $c = 15.8 \pm 2.0$ mM^{-1} s^{-1}
			V	7	$pK'_3 = 4.68 \pm 0.06$, $Y_L = 3.1 \pm 0.39$ s^{-1}, $Y_H = 51 \pm 2$ s^{-1}
	D_2O	3.7–6.3	V/K	6	$pK_1 = 4.1 \pm 0.1$, $pK_2 = 6.0 \pm 0.1$, $c = 15 \pm 2$ mM^{-1} s^{-1}
			V	7	$pK'_3 = 4.92 \pm 0.08$, $Y_L = 1.8 \pm 0.3$ s^{-1}, $Y_H = 23 \pm 1.0$ s^{-1}
AcRASQNYPVV-NH_2	H_2O	3.2–7.1	V/K	6	$pK_1 = 3.4 \pm 0.1$, $pK_2 = 6.20 \pm 0.09$, $c = 16 \pm 1.6$ mM^{-1} s^{-1}
			V	7	$pK'_3 = 5.0 \pm 0.16$, $Y_L = 13 \pm 2$ s^{-1}, $Y_H = 132 \pm 15$ s^{-1}
	D_2O	3.3–7.6	V/K	6	$pK_1 = 4.28 \pm 0.08$, $pK_2 = 6.64 \pm 0.08$, $c = 1.7 \pm 1.6$ mM^{-1} s^{-1}
			V	7	$pK'_3 = 5.64 \pm 0.06$, $Y_L = 9.6 \pm 0.3$ s^{-1}, $Y_H = 47 \pm 1.6$ s^{-1}
AcSQSYPVV-NH_2	H_2O	3.3–6.3	V/K	6	$pK_1 = 3.5 \pm 0.1$, $pK_2 = 6.1 \pm 0.1$, $c = 0.45 \pm 0.03$ mM^{-1} s^{-1}
			V	7	$pK'_3 = 4.2 \pm 0.6$, $Y_H = 2.11 \pm 0.095$ s^{-1}, $Y_L = 1.6 \pm 0.2$ s^{-1}
AcRKILFLDG-NH_2	H_2O	3.2–7.2	V/K	6	$pK_1 = 3.7 \pm 0.2$, $pK_2 = 6.5 \pm 0.2$, $c = 39 \pm 7$ mM^{-1} s^{-1}
			V	7	$pK'_3 = 4.2 \pm 0.2$, $Y_H = 4.3 \pm 0.3$ s^{-1}, $Y_L = 0.8 \pm 0.2$ s^{-1}

[a] Results obtained in 50 mM each of glycine, sodium acetate, Mes, and Tris [pH(D) = 3–7], 1 mM DTT, 1 mM EDTA, 200 mM NaCl, and 0.1% Triton X-100 prepared in H_2O or D_2O, containing variable concentrations of substrate and 18–120 ng of purified HIV-1 protease at 37 °C.

enzymatic groups of $pK = 4.9 \pm 0.06$ and 3.1 ± 0.1 must be deprotonated for this cationic inhibitor to bind (Table I). The pK_{is} profile for the uncharged inhibitor **2** similarly decreased below pH 4, but with an apparent slope of 1, and also decreased above pH 4 to a level at basic pH at which the inhibitor bound less tightly. Compound **2** does not bind to HIV-1 protease at low pH but does bind less tightly to the enzyme at pH values above the pH of its optimal binding. These data, fitted to eq 8, indicated that compound **2** binds to the protease when an enzymatic group of $pK_1 = 3.3 \pm 0.1$ was deprotonated and bound more tightly to the enzyme when a residue of $pK_2 = 5.3 \pm 0.09$ was protonated. The cationic inhibitor **1** binds only to a form of the protease in which both of these groups are unprotonated, while the uncharged inhibitor **2** binds to this enzyme form less favorably than one in which the residue of pK_2 is protonated and that of pK_1 is unprotonated.

(*b*) *Substrates.* The pH dependence of V/K and V were similarly investigated for four oligopeptide substrates of which these two kinetic parameters vary by as much as 50- and 120-fold, respectively (Hyland et al., 1991). Two of these substrates were examined in both H_2O and 88% D_2O. Shown in Table I are pK values determined from plots of log V/K and log V vs pH for the four substrates. Plots of log V/K vs pH for AcRASQNYPVV-NH_2 (Figure 2) and the other three substrates in H_2O were "bell-shaped", in which the value of log V/K decreased at acidic and basic pH with asymptotic slopes of 1 and −1, respectively. The pK values in Table I were obtained from fitting these data to eq 6. Similar to compound **2**, AcSQNYPVV-NH_2, AcRASQNYPVV-NH_2, and AcSQSYPVV-NH_2 bind to an enzyme form that contains an unprotonated catalytic group of $pK_1 = 3.4$–3.7 and a protonated catalytic group of $pK_2 = 5.5$–6.5. While these substrates possess no titratable groups in this pH range, the β-carboxyl group of the aspartyl residue of AcRKILFLDG-NH_2 would have a pK between 3 and 5, and the protonation state of this group may influence its ability to bind to the protease. Although slightly different values of pK were observed in the profile of log $V/K_{AcRKILFLDG\text{-}NH_2}$ than in the previous examples, an additional pK was not evident in this plot (data not shown). In a limited analysis, the variation of V/KE_t with variable pH (4.0–7.0) for Ac-Arg-Lys-Ile-Leu*(*p*-nitro)Phe-Leu-Asp-Gly-NH_2 by using a continuous spectrophotometric assay to measure initial rates (Tomaszek et al., 1990) appeared to be similar to that observed for the analogous substrate Ac-RKILFLDG-NH_2 using the stopped-time HPLC-based assay.

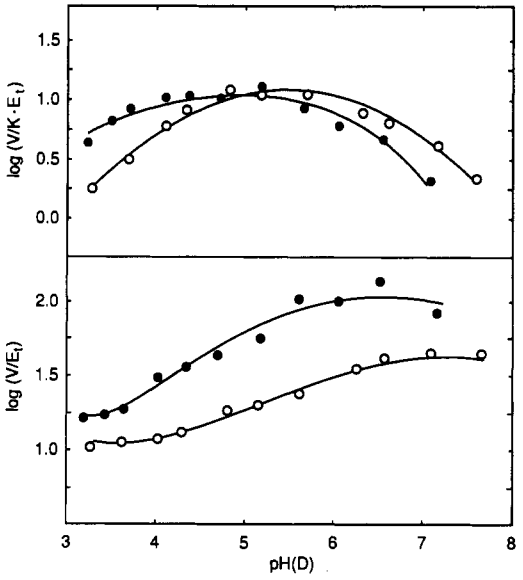

FIGURE 2: pH(D) rate profiles for AcRASQNYPVV-NH_2. V and V/K values were obtained from fitting of initial velocity data in H_2O (●) and 88% D_2O (○) at each value of pH(D) to eq 1. The curves drawn through the experimental points were obtained from fitting to eq 6 for V/K and eq 7 for V.

These results suggest that the use of the single-point stopped-time assay as performed here accurately reflects the pH dependence of initial peptidolytic rates.

For all four oligopeptide substrates, the profiles of log V vs pH were "wave-shaped" (fitted to eq 7) in which protonation of an enzymatic residue of $pK = 4.2$–5.2 shifted V to a constant lower value. The profile of log V vs pH for AcRASQNYPVV-NH_2 is shown in Figure 2. These profiles indicate that protonation of an enzymatic group in the enzyme–substrate (or an enzyme–product) complex results in a parallel, but slower, reaction pathway.

The profiles of log V/K and log V vs pD (in 88% D_2O) for AcSQNYPVV-NH_2 and AcRASQNYPVV-NH_2 are of similar shape to those obtained in H_2O (the pD profiles for AcRASQNYPVV-NH_2 are superimposed on the pH profiles in Figure 2). As the plots of log V/K and log V vs pD were fitted to the same respective equations as those of the corresponding pH profiles, the same titratable groups observed in the pH profiles appear in the pD profiles but with a shift in pK value due to the solvent equilibrium isotope effect (Table

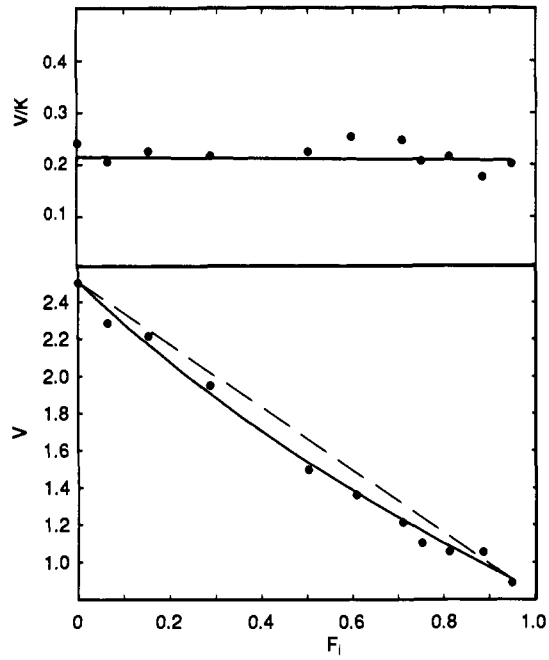

FIGURE 3: Proton inventory data for AcRASQNYPVV-NH_2 at pH(D) 6. Values of V/K and V were determined from fitting of initial velocity data to eq 1 at mole fractions (F_i) of D_2O of 0–0.96. The curves drawn through the experimental points were obtained from linear regression of V/K values and by fitting V values to eq 10. In the V profile, the upper and lower data points are connected by a straight dashed line to accentuate the curvature.

I). For the two substrates, the observed pK values are shifted to higher values in D_2O: ΔpK_1 = 0.5–0.8, ΔpK_2 = 0.5–0.6, and $\Delta pK_3'$ = 0.25–0.54, in accord with the expected value for the solvent equilibrium isotope effect on a carboxylate residue in 100% D_2O [ΔpK = 0.5–0.6 (Schowen, 1977)].

Solvent Kinetic Isotope Effects. As indicated from the data shown in Figure 2 and Table I, the solvent kinetic isotope effects were obtained for the oligopeptide substrates AcRASQNYPVV-NH_2 and AcSQNYPVV-NH_2 over a pH(D) range of 3–7 in which the isotopic solvent consisted of 88% (v/v) D_2O (F_i = 0.88). On the basis of the values of c, Y_L, and Y_H (Table I), the pH-independent values for AcRASQNYPVV-NH_2 and AcSQNYPVV-NH_2, respectively, were calculated to be $^DV/K$ = 1.0 ± 0.1 for both, $^DV_{low\ pH}$ = 1.5 ± 0.2 and 1.7 ± 0.3, and $^DV_{high\ pH}$ = 3.2 ± 0.4 and 2.2 ± 0.9. At neutral (high) pH, the apparent solvent isotope effect on V/K for either substrate was inverse, but at pH(D) ≤4, $^DV/K$ became normal (>1.0) in either case. In contrast, ^DV was large (2–3) for both substrates at neutral pH but decreased to lower values upon protonation of the enzymatic residue of pK = 4.5. A greater attentuation of ^DV was observed for the larger substrate, AcRASQNYPVV-NH_2, of which ^DV became 1.6 at pH(D) 3.2. At pH(D) 6.0, $^DV/K$ = 0.97 ± 0.06 and ^DV = 2.0 ± 0.3 for AcSQSYPVV-NH_2.

Proton inventories were conducted for AcSQNYPVV-NH_2 and AcRASQNYPVV-NH_2 at pH(D) 6.0. This value of pH(D) was chosen due to its displacement from the titratable group observed in the profile of log V vs pH(D), such that the apparent effects on V due to enrichment of the solvent with D_2O do not arise from an overt change in the active protomeric form of the enzyme due to the solvent equilibrium isotope effect. For either substrate, V/K was invariant with respect to increasing mole fraction of D_2O (F_i), as expected, while V decreased in a nonlinear fashion to produce concave ("bowl-shaped") plots of V vs F_i (Figure 3). A comparison of the linear regressions of plots of V vs F_i and $V^{1/2}$ vs F_i for either

Scheme I

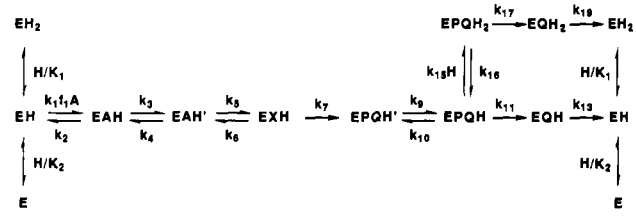

substrate revealed a better linear correlation for $V^{1/2}$ vs F_i. This result indicates a normal solvent kinetic isotope effect in which the fractionation factors of two protons are decreased in the transition state of the rate-limiting reaction step (Venkatasubban & Schowen, 1985; Schowen, 1977; Schowen, 1978). Each set of data of V vs F_i were fitted individually to eqs 9–11, which describe a transition state in which one, two, or three protons are transferred, respectively, with nonidentical isotope effects on each proton transfer step.

For AcRASQNYPVV-NH_2 (Figure 3) and AcSQNYPVV-NH_2 (data not shown) at pH(D) 6.0, the data from plots of V vs F_i were fitted best by eq 10 [for AcRASQNYPVV-NH_2, the correlation coefficients were 0.995 (eq 9), 0.998 (eq 10), and 0.997 (eq 11)]. For proton inventory data of this degree of solvent isotope effect, the discrimination between one-proton and two-proton mechanisms is generally more straightforward than distinguishing mechanisms that involve two or more protons (Schowen, 1978).[2] The present analysis indicates that the transition state of the rate-limiting step of peptidolysis of AcRASQNYPVV-NH_2 and AcSQNYPVV-NH_2 is best characterized by the simultaneous transfer of two protons. The fit of each of these data sets to eq 10 resulted in identical values of ϕ_1^T and ϕ_2^T: for AcRASQNYPVV-NH_2, $\phi_1^T = \phi_2^T$ = 0.57 ± 0.01; and, for AcSQNYPVV-NH_2, $\phi_1^T = \phi_2^T$ = 0.60 ± 0.04, which correspond to isotope effects of 1.75 (AcRASQNYPVV-NH_2) and 1.67 (AcSQNYPVV-NH_2) for each of the two transferred protons. At pH(D) 3.6, the plot of V vs F_i for AcSQNYPVV-NH_2 was best fitted to eq 10, from which $\phi_1^T = \phi_2^T$ = 0.74 ± 0.05 (data not shown).

Discussion

pH Studies. A minimal kinetic mechanism for HIV-1 protease that accounts for results of pH rate studies with substrates and inhibitors is shown in Scheme I, in which A is substrate concentration, H is proton concentration, P and Q are product concentrations [P = Ac(RA)SQNY and Q = PVV-NH_2], EAH′ and EPQH′ are conformational isomers of EAH and EPQH in which the substrate-binding "flaps" are closed, X is an enzyme-bound tetrahedral adduct of peptide and H_2O, $f_i = [EH]/E_t = 1/(1 + H/K_1 + K_2/H)$, K_1 = [EH][H]/[EH_2], K_2 = [E][H]/[EH], and $k_{16}/k_{15} = K_3$ = [EPQH][H]/[$EPQH_2$]. Since it has been shown that the "flaps" move significantly upon binding of a substrate analogue (inhibitor) to form the binding pockets (Miller et al., 1989),

[2] Equations 9–11 are specific forms of the more general equation, $k_n = k_0[\prod_j'(1 - n + n\phi_j^T)/\prod_j'(1 - n + n\phi_j^R)]$ (Kresge, 1964; Hunkapiller et al., 1976) in which ϕ_j^T and ϕ_j^R are isotope fractionation factors for the transition state and reactants, respectively, n is F_i, and ν (the number of protons transferred) = 1, 2, or 3. The denominator of this equation can be shown to be approximately equal to unity for exchangeable protons on enzymatic groups other than sulfhydryl groups (Venkatasubban & Schowen, 1985). In addition to the use of eqs 9–11, one can alternatively calculate the number of protons transferred (ν) by using $V_n = V_0(1 - F_i + F_i\phi_n^T)^\nu$ in which one assumes that ϕ_i^T is identical for each transferred proton. Solution of this equation with the data of Figure 3 resulted in values of ϕ_n^T = 0.6 ± 0.1 and ν = 2.2 ≙ 0.8.

it seems reasonable to include the EAH′ and EPQH′ complexes in the kinetic description of substrate hydrolysis, although, at present, no evidence exists for these conformational changes on the catalytic pathway. Given initial velocity conditions and the inability to observe a reverse peptidolytic reaction or isotope exchange as described in the accompanying paper (Hyland et al., 1991), reaction steps defined by k_7, k_{11}, k_{13}, k_{17}, and k_{19} are effectively irreversible.

From the pH profiles of the competitive inhibitors (Figure 1), the cationic inhibitor **1** binds only to the fully unprotonated enzyme form E of Scheme I, while the neutral inhibitor **2** binds most tightly to the monoprotonated enzyme form EH. Neither inhibitor binds to the diprotonated form EH_2 and **1** binds only to E. The average values of $pK_1 = 3.2$ and $pK_2 = 5.1$ obtained from these plots indicate the acid dissociation constants of the catalytic aspartyl groups in the active site.

For HIV-1 protease, the oligopeptide substrates only bind to EH, and subsequent to the k_7 step, protonation of an enzyme–product complex (for simplicity, defined here as EPQH) elaborates a slower parallel path of product release. Expressions for V/K and V derived for this kinetic scheme are given by eqs 12 and 13, respectively. In fact, protonation of any enzyme form from among EAH, EAH′, EPQH′, EPQH, and EQH would give rise to the observed pH-dependent behavior of log V/K and log V, but presumably the EAH and EPQH complexes, in which the substrate-binding flaps are in their "open" forms, are the two most likely complexes in which the active site is accessible to solvent. The protonation of the EAH complex to elaborate the parallel reaction pathway cannot be excluded by the available data. Presumably, protonation of an active-site aspartyl group in EAH would result in a chemical mechanism in which both aspartyl groups are protonated.[3]

$$V/K = \frac{k_1k_3k_5k_7E_t}{[k_2k_4(k_6 + k_7) + (k_2 + k_3)k_5k_7](1 + H/K_1 + K_2/H)} \quad (12)$$

$$V = \frac{[V_L + V_H(K_3'/H)]E_t}{1 + K_3'/H} \quad (13)$$

in which

$$V_L = [k_3k_5k_7E_t]/[(k_3 + k_4)(k_6 + k_7) + k_3k_5k_7[1/k_3 + 1/k_7 + (k_{10} + k_{11})/k_9k_{11} + 1/k_{17} + 1/k_{19}]] \quad (14)$$

$$V_H = [k_3k_5k_7E_t]/[(k_3 + k_4)(k_6 + k_7) + k_3k_5k_7[1/k_3 + 1/k_7 + (k_{10} + k_{11})/k_9k_{11} + 1/k_{11} + 1/k_{13}]] \quad (15)$$

$$K_3' = K_3(V_L/V_H)[k_{11}(k_{16} + k_{17})/k_{16}k_{17}] \quad (16)$$

Equation 12 is of the same form as eq 6 and describes a "bell-shaped" profile for log V/K vs pH. The values for pK_1 and pK_2 should be equal to those observed in pH profiles of the competitive inhibitors, regardless of the extent of "stickiness"[4] of the substrates (Cleland, 1977). The pK_1 values of 3.5–3.7 obtained in the substrate profiles are in good agreement with those found in the inhibitor profiles (3.1–3.3; $\Delta pK = 0.2$–0.4). The consistency of the pK_1 values is notable compared to the other aspartic proteases [e.g., penicillopepsin (Hofman et al., 1984)], and the agreement persists despite the considerable range of V/K values (about 100-fold) observed for the four oligopeptide substrates. However, with the exception of AcSQNYPVV-NH_2 ($pK_2 = 5.5$), the corresponding pK_2 values for the other substrates ($pK_2 = 6.1$–6.5) are displaced to considerably higher values than the "true" values obtained from the inhibitor profiles (average $pK_2 = 5.2$). This outward displacement of the pK_2 values of these other substrates would be expected upon the formation of a kinetically competent EA complex in Scheme I. Given that log V is unaffected in this pH range, this would result in the flattening of the log V/K profile, similar to that observed in the log V profiles, at pH values above pK_2 such that the profile would conform to that described by eq 8. While the instability of the protease precluded the acquisition of reliable data above pH 7 to explore this possibility more thoroughly, none of the data in the available log V/K profiles in Table I were fitted by eq 8 better than by eq 6. In their pH rate studies of the HIV-1 protease using the chromophoric substrate, Lys-Ala-Arg-Val-Leu-(*p*-nitro)Phe-Glu-Ala-Nle-Gly-NH_2 (Nle = norleucinyl), Richards et al. (1990) found that the log V/K profile became flattened above a pK of 5.7 in which the corresponding log V was invariant over the pH range studied. This may indicate that the EA complex is kinetically competent with some oligopeptide substrates.

Equation 13 is analogous to eq 7 and describes a "wave-shaped" pattern for log V vs pH in which the pK_3' value is an apparent value of the acid dissociation constant pK_3 and is defined by the ratio of V values obtained at the plateaus of low and high pH and by the partitioning between the EPQH and $EPQH_2$ complexes [given by $[k_{11}(k_{16} + k_{17})]/k_{16}k_{17}$]. As is inherent from the proposed mechanism in Scheme I, the observed shifting of V to lower values at low pH values is due solely to the retardation of product release steps upon protonation of an enzyme-product complex ($1/k_{17} + 1/k_{19} > 1/k_{11} + 1/k_{13}$). However, the protonation step could precede the isomerization of the EPQH′ complex (before the k_9 step) without alteration of the form of eq 13. The simultaneous observation of a "bell-shaped" V/K profile and "wave-shaped" V profile has been reported for the glucose 6-phosphate dehydrogenase of *Leuconostoc mesenteroides*, which has been interpreted in terms of a mechanism similar to that of Scheme I (Viola, 1984).

The enzyme forms to which the competitive inhibitors bind reveal additional details about the protonation states of the active-site aspartyl groups. Inhibitors **1** and **2** both contain moieties bearing tetrahedral carbon atoms that are isosteric surrogates of the scissile dipeptide bond of the oligopeptide substrates. Compound **2**, as do the oligopeptide substrates, preferentially binds to the monoprotonated enzyme species, which suggests that the formation of the tetrahedral amide hydrate (enzyme species EXH) requires both a protonated and unprotonated aspartyl group in the active site. This conclusion is supported by structural analysis of a complex of HIV-1 protease and a hydroxyethylene-containing inhibitor (Jaskolski et al., 1991). However, the cationic compound **1** can only bind to the enzyme form E in which both aspartyl residues are

[3] Whether it is the EAH or the EPQH complex that is protonated in the log V profile cannot be distinguished kinetically. The pH rate data and the solvent kinetic isotope effects can be interpreted in support of either case. However, catalysis by the two protonated aspartyl residues within the putative EAH_2 complex could be envisioned by three subsequent steps involving proton transfers: (1) protonation of the scissile carbonyl oxygen by Asp-25, (2) deprotonation of Asp-25′ by Asp-25, and (3) deprotonation of the lytic water by Asp-25′ and attack of the resulting hydroxide ion on the protonated carbonyl group. Inconsistent with such a mechanism is proton inventory data, which indicates the concerted transfer of two protons in the transition state at pH(D) 3.6. In addition, the tighter binding of AcSQNY to EQH at pH 3.5 (Hyland et al., 1991). supports a slower mechanistic pathway resulting from protonation of the EPQH complex.

[4] A "sticky" substrate is one that reacts to yield products faster than it dissociates from the enzyme (Cleland, 1977).

unprotonated, and it is likely then that this inhibitor forms an ionic bond with the β-carboxylate ion of an aspartyl residue (Asp-25′ in Figure 4), which is normally protonated in the catalytically competent enzyme form. Binding of **1** to this improper enzyme form may help account for its relatively poor inhibition constant at the pH optimum of the protease. The nature of this enzyme–inhibitor complex suggests that the amine which departs from the initial tetrahedral intermediate is probably protonated by Asp-25′.

In the three-dimensional structure of an HIV-1 protease–inhibitor complex solved at 2.3-Å resolution (Miller et al., 1989), the hexapeptide inhibitor, which contains a "reduced amide" isostere similar to that of compound **1**, binds in an extended conformation in the active-site cleft. The nitrogen atom of the $-CH_2NH-$ isosteric group is proximal to the two oxygen atoms of one of the catalytic aspartyl residues. The inability of the protonated reduced amide inhibitor **1** to bind to enzyme when this aspartyl group is protonated cannot be explained entirely by poor electrostatic interactions but may instead be due to steric repulsion between the protons on the inhibitor and the aspartyl group. Compared to the structure of the uncomplexed protease, binding of this inhibitor causes the symmetric "flaps" (amino acids 48–52 and 48′–52′) to move by 7 Å and close down around the bound inhibitor, thereby forming the substrate binding sites. As a result, the catalytic aspartyl groups are likely to be inaccessible to solvent in the protease–inhibitor complex. This may explain in part the absence of those pK's observed in the log V/K profiles from the log V profiles.

Analysis of Solvent Kinetic Isotope Effects. Assuming that the chemical mechanism of HIV-1 protease involves a single important enzyme-bound reaction intermediate (namely, the amide hydrate), one would expect the k_5 and k_7 reaction steps in Scheme I to be isotope sensitive in that the formation and breakdown of the EXH complex should involve proton transfers. Expressions for the solvent kinetic isotope effects on V/K and V for the peptidolytic reaction of HIV-1 protease are given by

$$^{D}V/K = \frac{^{D}K_{eq5}{}^{D}k_7 + k_7/k_6[^{D}k_5 + k_5/k_4(1 + k_3/k_2)]}{1 + k_7/k_6[1 + k_5/k_4(1 + k_3/k_2)]} \quad (17)$$

$$^{D}V = [^{D}k_7 + {}^{D}k_7{}^{D}K_{eq5}k_6(k_3 + k_4)/k_3k_5 + k_7[1/k_3 + {}^{D}k_5(k_3 + k_4)/k_3k_5 + (k_{10} + k_{11})/k_9k_{11} + a]]/[1 + k_7[1/k_3 + (k_3 + k_4)(1 + k_6/k_7)/k_3k_5 + (k_{10} + k_{11})/k_9k_{11} + a]] \quad (18)$$

in which $a = 1/k_{17} + 1/k_{19}$ and $1/k_{11} + 1/k_{13}$ at low and high pH, respectively.

For the substrates AcRASQNYPVV-NH_2 and AcSQNYPVV-NH_2, $^{D}V/K$ = 1.0 and ^{D}V = 3.2 and 2.2, respectively, at high pH(D), while, at pH(D) <4, ^{D}V decreases (becomes 1.6 for AcRASQNYPVV-NH_2). The absence of an isotope effect on V/K results from a high forward commitment [$c_f = k_7/k_6(1 + k_5/k_4(1 + k_3/k_2)) = 12.5$, Hyland et al. (1991)]. This attentuation of the isotope effect on V/K is not relieved by using the poorer, and possibly less "committed", substrate AcSQSYPVV-NH_2 (V/K is 1.3% that of AcSQNYPVV-NH_2 and AcRASQNYPVV-NH_2). Values of $^{D}V/K$ and ^{D}V for AcSQSYPVV-NH_2, 0.97 and 2.0, respectively, at pH(D) 6.0 were similar to those of the more competent peptide substrates.

The observed expression of normal and inverse isotope effects on V/K at low and high pH(D), respectively, does not reflect the pH-dependent attenuation of the forward commitment since the mechanism in Scheme I predicts that the peptide substrates bind only to the correctly protonated enzyme form EH and chemical steps cannot be made fully rate-limiting at a nonoptimal value of pH(D) (Cook & Cleland, 1981). Rather, the nonunity values of $^{D}V/K$ at high and low pH(D) result from the solvent equilibrium isotope effect expressed on the values of pK_1 and pK_2 (Schowen, 1977). Therefore, the parameter $^{D}V/K$ is not truly pH(D)-dependent, and the attentuation of $^{D}V/K$ by a high forward commitment, c_f, is not relieved at a catalytically unfavorable pH(D). If we attribute the isomerization step (k_3) to binding of the flaps to the bound substrate, designated by the EAH–EAH′ isomerization in Scheme I, it is reasonable to assume that the substrate is extremely sticky in the EAH′ complex ($k_5/k_4 > 10$), which would account for a large value of c_f. An examination of eq 17 indicates that, at c_f = 12.5, $^{D}V/K$ would be unity when the k_7/k_6 value is low. By use of fractionation factors as tabulated by Schowen (1977), a value of 0.64 can be calculated for $^{D}K_{eq5}$. Assuming values for k_3/k_2, k_5/k_4, k_7/k_6, $^{D}k_5$, and $^{D}k_7$ of 2.0, 40, 0.1, 4.0, and 4.0, respectively, from eq 17, a value of 1.1 is calculated for $^{D}V/K$, in good agreement with the experimentally determined value of 1.0 ± 0.1.

The values of ^{D}V of 2–3 for AcRASQNYPVV-NH_2, AcSQSYPVV-NH_2, and AcSQNYPVV-NH_2 indicate that a proton transfer step (or steps) is (are) at least partly rate-limiting for these substrates at pH(D) 5–6. The rate-limiting proton-transfer step occurs either in the formation (k_5) or breakdown (k_7) of the enzyme-bound tetrahedral adduct of substrate and H_2O (EXH). The observation of exchange of ^{18}O into substrate from H_2O (Hyland et al., 1991) indicates that the breakdown of the EXH complex occurs more slowly than its reversible formation, implicating the k_7 reaction step as rate-limiting to catalysis. From the proton inventory data, this step involves the simultaneous transfer of at least two protons in the transition state.

As indicated in Scheme I, protonation of an enzymatic residue of pK_3 in an enzyme–product complex slows down catalysis due to an apparent change in rate-limiting step for the protease-catalyzed reaction. The decrease in ^{D}V at low pH(D) for the substrates AcRASQNYPVV-NH_2 and AcSQNYPVV-NH_2 suggests that this is due to a retardation of nonchemical steps, such as a conformational change or the release of products (the a term in eq 18 becomes large as product-release steps become rate-limiting, thereby lowering the expression of the intrinsic isotope effects $^{D}k_5$ and $^{D}k_7$ on ^{D}V). For AcRASQNYPVV-NH_2, ^{D}V decreases from 3.0 to 1.6 as pH(D) goes from 6.0 to 3.2, indicating that nonchemical steps become almost totally rate-limiting at low pH(D).

The identity of the enzymatic group of pK_3 and the effect of its protonation on the suppression of product-release steps remains unclear. The complexity of the expression for pK_3' (eq 16) does not allow the calculation of pK_3, although division of the pK_3' values (Table I) by the corresponding values of V_H/V_L results in the normalized values of $-\log [K_3k_{11}(k_{16} + k_{17})/(k_{16}k_{17})]$, which range from 3.5 to 4.9. The enzymatic group of pK_3 is most probably a carboxylic residue and could be Asp-25′, which putatively imparts the proton it received from the lytic H_2O to the amine nitrogen (Figure 4). One would expect protonation of Asp-25′ to be more facile in the EPQH complex, in which the "flaps" have opened to allow the release of the products, than in the "closed" EPQH′ complex, which is likely to be solvent inaccessible. The pK of this Asp-25′ group in the free enzyme is 3.2, but this value may be perturbed when the active site is occupied and the proton on Asp-25 is not oriented to hydrogen bond to Asp-25′. Given

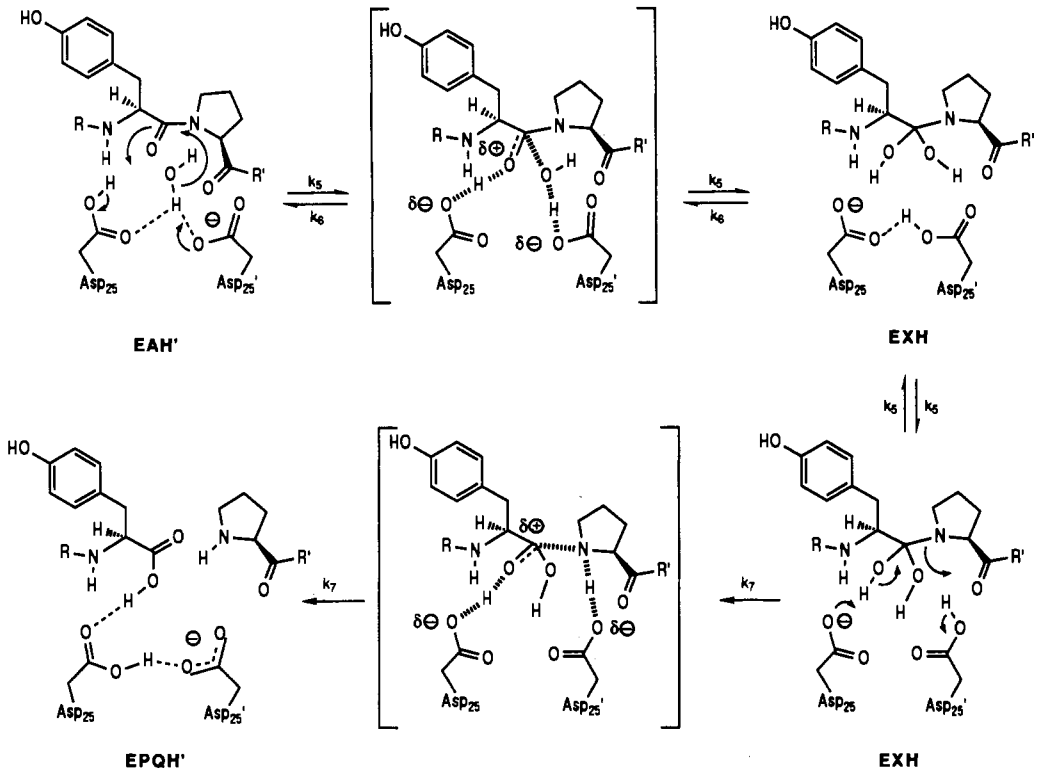

FIGURE 4: Proposed chemical mechanism of the peptidolytic reaction of HIV-1 protease based on kinetic and structural data. The enzyme complexes cited are those depicted in Scheme I. Proposed hydrogen bonds are indicated by dashed lines and are based in part on molecular modeling of the enzyme–intermediate complex in the accompanying paper.

the potentially close contacts between the β-carboxylate group of this active-site residue and the amino group of the product as indicated above, the departure of the neutral amine product from the EPQH complex might be accelerated by electrostatic repulsion between the lone pair electrons of the amine and the β-carboxylate of Asp-25′. If the solvent is accessible to the buried Asp-25′ residue in the EPQH complex, protonation of Asp-25′ would retard the desorption of the amine due to potential hydrogen bonding to the carboxylic acid or due to the formation of an ionic bond upon protonation of the amine. Otherwise, the protonation of a more accessible residue that is structurally important to the enzyme, such as Asp-29, (Wlodawer et al., 1989), could effect a protein conformational change that affects product release or "flap" movement steps. The substrate-binding "flap" regions of the enzyme contain no acidic residues.

Chemical Mechanism. In Figure 4 is a proposed chemical mechanism for HIV-1 protease that is based on the present kinetic data as well as structural data for HIV-1 protease (Wlodawer et al., 1989; Miller et al., 1989; Swain et al., 1990) and the analogous aspartic proteases, penicillopepsin (Suguna et al., 1987; James & Sielecki, 1985) and rhizopuspepsin (Bott et al., 1982). The mechanism outlined in Figure 4 is consistent with all of the kinetic data in this report and its companion (Hyland et al., 1991) and has many features in common with the general acid–general base mechanisms proposed for the aspartic proteases by James et al. (1977), Bott et al. (1985), Rich (1985), and Suguna et al. (1987) and, in particular, the "push–pull" mechanism proposed by Polgar (1987).

In the free enzyme complex to which substrates bind (EH), the proton on the β-carboxylate of Asp-25 (pK_2 = 5.1) is likely to be hydrogen bonded to the anionic β-carboxylate of Asp-25′ (pK_1 = 3.2). Upon binding of substrate, isomerization of the binary EAH complex to the EAH′ complex is tantamount to the closing of the flaps down around the bound substrate. We propose that during the binding of the substrate, the proton on Asp-25 is positioned to hydrogen bond to the carbonyl oxygen of the substrate, and, at the same time, the lytic H_2O is positioned closer to the β-carboxylate of Asp-25′. The loss of the shared proton from Asp-25 should render the β-carboxylic group of Asp-25′ more basic than in the free enzyme, as suggested by Bott et al. (1982) for rhizopuspepsin, thereby facilitating proton abstraction from the lytic water. Suguna et al. (1987) have made a similar argument from their crystallographic analysis of a penicillopepsin–inhibitor complex.

Abstraction of a proton from the lytic H_2O molecule by Asp-25′ and the attack of the resulting hydroxide ion upon the carbonyl of the scissile dipeptide bond occurs simultaneously with protonation of the carbonyl oxygen by Asp-25. The concerted transfer of two protons in the transition state of the k_5 step results in the formation of an enzyme-bound amide hydrate (EXH complex). The formation of this intermediate, as opposed to an oxyanionic intermediate that occurs in the mechanism of the serine proteases, is supported by the observation that the protease is able to abstract either of the two oxygen atoms of this intermediate as H_2O, as evidenced by ^{18}O exchange into the substrate. This indicates that the two oxygen atoms in the enzyme-bound intermediate are, in effect, chemically equivalent and further exemplifies the symmetrical disposition of the aspartyl residues in the enzyme's active site, which may freely transfer their shared proton, as well as the symmetrical nature of the amide hydrate intermediate itself.

Upon formation of the EXH complex, the protonation states of the two aspartic residues are now opposite to those in the free enzyme. Given that ^{18}O may be exchanged from H_2O into re-formed substrate, the formation and reversal of the EXH complex must be faster than its breakdown to products (in fact, may come to equilibrium on the enzyme), such that the k_7 step should be the rate-limiting catalytic step. Proton inventory data indicate that two protons are transferred in the transition state of this rate-limiting step, and, at best determination, the values of the isotope effects of the individual

proton transfers are equal. This suggests that the collapse of the tetrahedral intermediate of EXH occurs through a transition state in which transfer of a proton from the amide hydrate to Asp-25 is concerted with, and to an equal extent as, the transfer of proton from Asp-25′ to the nitrogen atom of the departing proline. The proton inventory data reported here for HIV-1 protease are similar to those reported for the peptidolytic reaction of α-lytic protease, for which an analogous transition state has been proposed (Hunkapiller et al., 1976). In the "two-proton" mechanism of this serine protease, one proton is transferred from an aspartyl residue to N_π of the catalytic histidinyl residue simultaneously with the equally extended transfer of a proton from the N_τ of the histidine to an incipient amine, which results from the collapse of a tetrahedral adduct of peptide substrate and the active-site serine. The chemical mechanism proposed here for HIV-1 protease resembles in part that which has been recently advanced by Jaskolski et al. (1991), from structural analysis of a protease–inhibitor complex, in that the amine product is protonated by an active-site aspartyl residue. However, these authors favor a concerted mechanism in which the attack of the nucleophilic water on the scissile carbonyl is simultaneous with the protonation of the amine and cleavage of the C–N bond, such that no discrete enzyme-bound intermediate is formed.

That the collapse of the enzyme-bound amide hydrate is apparently rate-limiting for catalysis by HIV-1 protease suggests that the potency of peptide analogue inhibitors of this enzyme that contain tetrahedral isosteric replacements of the scissile peptide bond may depend on the fidelity of mimicry of the second transition state in Figure 4, as opposed to the amide hydrate intermediate itself. Rich and co-workers have recently reported a peptide analogue inhibitor of HIV-1 protease that contains a hydroxyethylamine isostere [Ac-Ser-Leu-Asn-Pheψ(CHOHCH$_2$N)Pro-Ile-Val-OMe, K_i = 0.66 nM; Rich et al. (1990)]. While this inhibitor is a structural "composite" of inhibitors **1** and **2**, it is considerably more potent. The separation of the protonated proline nitrogen from the hydroxyl-bearing tetrahedral carbon atom by the presence of an additional methylene group, as compared to its absence in **1** and **2**, may better mimic the second (rate-limiting) transition state in Figure 4 in which the scission of the carbon–nitrogen bond may have occurred to a considerable extent. In support of this view, X-ray crystallographic analysis of a complex of this hydroxyethylamine inhibitor and HIV-1 protease indicates hydrogen-bonding contacts between the hydroxyl group and the β-carboxylic groups of the active-site aspartyl residues, one of which is within hydrogen-bonding distance to the proline nitrogen (Swain et al. 1990).

Acknowledgments

We thank Professors Paul F. Cook and W. W. Cleland for helpful discussions and Professor Cook for critical reading of the manuscript. We thank Dr. Jeffrey Culp, Dr. James E. Strickler, Ms. Joselina Gorniak, and Mr. Michael Minnich for providing purified HIV-1 protease and Drs. Michael L. Moore and Geoffrey B. Dreyer for providing substrates and inhibitors. We thank Dr. Brian W. Metcalf for continuing support of this research and for helpful discussions.

References

Bott, R., Subramanian, E., & Davies, D. R. (1982) *Biochemistry 21*, 6956–6962.

Cleland, W. W. (1963) *Biochim. Biophys. Acta 67*, 104-137.

Cleland, W. W. (1977) *Adv. Enzymol. Relat. Areas Mol. Biol. 45*, 273–387.

Cleland, W. W. (1979) *Methods Enzymol. 63*, 103–137.

Clement, G. E. (1973) *Prog. Bioorg. Chem. 2*, 177–238.

Clement, G. E., Snyder, S. L., Price, H., & Cartmell, R. (1968) *J. Am. Chem. Soc. 90*, 5603–5610.

Cook, P. F., & Cleland, W. W. (1981) *Biochemistry 20*, 1797–1805.

Cornish-Bowden, A. J., & Knowles, J. R. (1969) *Biochem. J. 113*,. 353–362.

Dreyer, G. B., Metcalf, B. W., Tomaszek, T. A., Jr., Carr, T. J., Chandler, A. C., III, Hyland, L. J., Fakhoury, S. A., Magaard, V. W., Moore, M. L., Strickler, J. E., Debouck, C., & Meek, T. D. (1989) *Proc. Natl. Acad. Sci. U.S.A. 86*, 9752–9756.

Fruton, J. S. (1987) in *Hydrolytic Enzymes* (Neuberger, A., & Brocklehurst, K., Eds.) pp 1–38, Elsevier, Amsterdam.

Green, D. W., Ayknet, S., Gierse, J. K., & Zupec, M. E. (1990) *Biochemistry 29*, 3126–3133.

Hofmann, T., Hodges, R. S., & James, M. N. (1984) *Biochemistry 23*, 635–643.

Hunkapiller, M. W., & Richards, J. H. (1972) *Biochemistry 11*, 2829–2839.

Hunkapiller, M. W., Forgac, M. D., & Richards, J. H. (1976) *Biochemistry 15*, 5581–5588.

Hyland, L. J., Tomaszek, T. A., Jr., Roberts, G. D., Carr, S. A., Magaard, V. W., Bryan, H. L., Fakhoury, S. A., Moore, M. L., Minnich, M. D., Culp, J. S., DesJarlais, R. L., & Meek, T. D. (1991) *Biochemistry* (preceding paper in this issue).

James, M. N. G., & Sielecki, A. R. (1985) *Biochemistry 24*, 3701–3713.

James, M. N. G., Hsu, I.-N., & Delbaere, L. T. J. (1977) *Nature (London) 267*, 808–813.

Jaskolski, M., Tomasselli, A. G., Sawyer, T. K., Staples, D. G., Heinrikson, R. L., Schneider, J., Kent, S. B. H., & Wlodawer, A. (1991) *Biochemistry 30*, 1600–1609.

Kostka, V. (1985) in *Aspartic Proteinases and Their Inhibitors* (Kostka, V., Ed.) Walter de Gruyter, Berlin.

Kresge, A. J. (1964) *Pure Appl. Chem. 8*, 243–258.

Lapatto, R., Blundell, T., Hemmings, A., Overington, J., Wilderspin, A., Wood, S., Merson, J. R., Whittle, P. J., Danley, D. E., Geoghegan, K. F., Hawrylik, S. J., Lee, S. E., Scheld, K. G., & Hobart, P. M. (1989) *Nature (London) 342*, 299–302.

Marquardt, D. W. (1983) *J. Soc. Ind. Appl. Math. 11*, 431–441.

Meek, T. D., Dayton, B. D., Metcalf, B. W., Dreyer, G. B., Strickler, J. E., Gorniak, J. G., Rosenberg, M., Moore, M. L., Magaard, V. W., & Debouck, C. (1989) *Proc. Natl. Acad. Sci. U.S.A. 86*, 1841–1845.

Miller, M., Schneider, J., Sathyanarayana, B. K., Toth, M. V., Marshall, G. R., Clawson, L., Selk, L., Kent, S. B. H., & Wlodawer, A. (1989) *Science 246*, 1149–1152.

Moore, M. L., Bryan, W. M., Fakhoury, S. A., Magaard, V. W., Huffman, W. F., Dayton, B. D., Meek, T. D., Hyland, L., Dreyer, G. B., Metcalf, B. W., Strickler, J. E., Gorniak, J., & Debouck, C. (1989) *Biochem. Biophys. Res. Commun. 159*, 420–425.

Navia, M. A., Fitzgerald, P. M. D., McKeever, B. M., Leu, C.-T., Heimbach, J. C., Herber, W. K., Sigal, I. S., Darke, P. L., & Springer, J. P. (1989) *Nature (London) 337*, 615–620.

Northrop, D. B. (1977) in *Isotope Effects in Enzyme-Catalyzed Reactions* (Cleland, W. W., O'Leary, M. H., & Northrop, D. B., Eds.) p 122, University Park Press, Baltimore, MD.

Pearl, L. H., & Taylor, W. R. (1987) *Nature (London)* 329, 351-354.
Polgar, L. (1987) *FEBS Lett. 219*, 1-4.
Polgar, L. (1989) *Mechanisms of Protease Action*, pp 157-182, CRC Press, Inc., Boca Raton, FL.
Rich, D. H. (1985) *J. Med. Chem. 28*, 263-273.
Rich, D. H., Green, J., Toth, M. V., Marshall, G. R., & Kent, S. B. H. (1990) *J. Med. Chem. 33*, 1285-1288.
Richards, A. D., Phylip, L. H., Farmerie, W. G., Scarborough, P. E., Alvarez, A., Dunn, B. M., Hirel, P.-H., Konvalinka, J., Strop, P., Pavlickova, L., Kostka, V., & Kay, J. (1990) *J. Biol. Chem. 265*, 7733-7736.
Schowen, K. B. J. (1978) in *Transition State of Biochemical Processes* (Gandour, R. D., & Schowen, R. L., Eds.) pp 225-279, Plenum Press, New York.
Schowen, R. L. (1977) in *Isotope Effects in Enzyme-Catalyzed Reactions* (Cleland, W. W., O'Leary, M. H., & Northrop, D. B., Eds.) pp 64-99, University Park Press, Baltimore, MD.
Suguna, K., Padlan, E. A., Smith, C. W., Carlson, W. D., & Davies, D. R. (1987) *Proc. Natl. Acad. Sci. U.S.A. 84*, 7009-7013.
Swain, A. L., Miller, M. M., Green, J., Rich, D. H., Kent, S. B. H., & Wlodawer, A. (1990) *Proc. Natl. Acad. Sci. U.S.A. 87*, 8805-8809.
Tang, J., Ed. (1977) *Acid Proteases, Structure, Function, and Biology*, pp 61-81, Plenum Press, New York.
Tomaszek, T. A., Jr., Magaard, V. W., Bryan, H. G., Moore, M. L., & Meek, T. D. (1990) *Biochem. Biophys. Res. Commun. 168*, 274-280.
Venkatasubban, K. S., & Schowen, R. L. (1985) *CRC Crit. Rev. Biochem. 17*, 1-41.
Viola, R. E. (1984) *Arch. Biochem. Biophys. 228*, 415-424.
Wlodawer, A., Miller, M., Jaskolski, M., Sathyanarayana, B. K., Baldwin, E., Weber, I. T., Selk, L. M., Clawson, L., Schneider, J., & Kent, S. B. H. (1989) *Science 245*, 616-621.

Catalytic Enhancement of Human Carbonic Anhydrase III by Replacement of Phenylalanine-198 with Leucine†

Philip V. LoGrasso,‡ Chingkuang Tu,‡ David A. Jewell,§ George C. Wynns,‡ Philip J. Laipis,§ and David N. Silverman*,‡

Department of Pharmacology and Therapeutics and Department of Biochemistry and Molecular Biology, University of Florida College of Medicine, Gainesville, Florida 32610

Received March 13, 1991; Revised Manuscript Received May 17, 1991

ABSTRACT: Carbonic anhydrase III, a cytosolic enzyme found predominantly in skeletal muscle, has a turnover rate for CO_2 hydration 500-fold lower and a K_I for inhibition by acetazolamide 700-fold higher (at pH 7.2) than those of red cell carbonic anhydrase II. Mutants of human carbonic anhydrase III were made by replacing three residues near the active site with amino acids known to be at the corresponding positions in isozyme II (Lys-64 → His, Arg-67 → Asn, and Phe-198 → Leu). Catalytic properties were measured by stopped-flow spectrophotometry and ^{18}O exchange between CO_2 and water using mass spectrometry. The triple mutant of isozyme III had a turnover rate for CO_2 hydration 500-fold higher than wild-type carbonic anhydrase III. The binding constants, K_I, for sulfonamide inhibitors of the mutants containing Leu-198 were comparable to those of carbonic anhydrase II. The mutations at residues 64, 67, and 198 were catalytically independent; the lowered energy barrier for the triple mutant was the sum of the energy changes for each of the single mutants. Moreover, the triple mutant of isozyme III catalyzed the hydrolysis of 4-nitrophenyl acetate with a specific activity and pH dependence similar to those of isozyme II. Phe-198 is thus a major contributor to the low CO_2 hydration activity, the weak binding of acetazolamide, and the low pK_a of the zinc-bound water in carbonic anhydrase III. Intramolecular proton transfer involving His-64 was necessary for maximal turnover.

Carbonic anhydrase III is a major protein of skeletal muscle where it comprises as much as 20% of cytosolic protein (Gros & Dodgson, 1988). Carbonic anhydrase II is found in red cells and secretory tissues. These isozymes of carbonic anhydrase are useful for investigations of catalytic mechanisms using site-directed mutagenesis because they have large differences in activity with very similar backbone structures. Isozyme III of carbonic anhydrase has a steady-state turnover number, k_{cat}, for hydration of CO_2 that is 500-fold smaller than that of isozyme II, and the binding constant for inhibition by acetazolamide is much weaker for isozyme III compared with isozyme II (Sanyal et al., 1982; Tu et al., 1983; Kararli & Silverman, 1985; Engberg et al., 1985). Moreover, isozyme III has a pK_a for the main activity-controlling group, zinc-bound water, that is lower by at least 1 pK_a unit compared

† This work was supported by a grant from the National Institutes of Health (GM 25154).
* Address correspondence to this author at the Department of Pharmacology and Therapeutics, Box J-267, Health Center, University of Florida, Gainesville, FL 32610-0267.
‡ Department of Pharmacology and Therapeutics.
§ Department of Biochemistry and Molecular Biology.

0006-2960/91/0430-8463$02.50/0